REPORT DOCUMENTATION PAGE

Form Approved
OMB No. 0704-0188

1. REPORT DATE *(DD-MM-YYYY)*	2. REPORT TYPE	3. DATES COVERED *(From - To)*
13-06-2008	Technical Paper	

4. TITLE AND SUBTITLE

Development of a Specific Impulse Balance for a Pulsed Capillary Discharge (Preprint)

5a. CONTRACT NUMBER

5b. GRANT NUMBER

5c. PROGRAM ELEMENT NUMBER

6. AUTHOR(S)
T.C. Lilly & A.P. Pancotti (ERC); A.D. Ketsdever, M. Young, & J.A. Duncan (AFRL/RZSA)

5d. PROJECT NUMBER

5e. TASK NUMBER

5f. WORK UNIT NUMBER
50260568

7. PERFORMING ORGANIZATION NAME(S) AND ADDRESS(ES)

Air Force Research Laboratory (AFMC)
AFRL/RZSA
10 E. Saturn Blvd.
Edwards AFB CA 93524-7680

8. PERFORMING ORGANIZATION REPORT NUMBER

AFRL-RZ-ED-TP-2008-223

9. SPONSORING / MONITORING AGENCY NAME(S) AND ADDRESS(ES)

Air Force Research Laboratory (AFMC)
AFRL/RZS
5 Pollux Drive
Edwards AFB CA 93524-7048

10. SPONSOR/MONITOR'S ACRONYM(S)

11. SPONSOR/MONITOR'S NUMBER(S)
AFRL-RZ-ED-TP-2008-223

12. DISTRIBUTION / AVAILABILITY STATEMENT

Approved for public release; distribution unlimited (PA #08237A).

13. SUPPLEMENTARY NOTES
For presentation at the 44th AIAA Joint Propulsion Conference, Hartford, CT, 20-23 July 2008.

14. ABSTRACT

A capillary discharge based pulsed plasma thruster is currently under development at the Air Force Research Laboratory. A torsion thrust stand has been developed to simultaneously measure the shot by shot total impulse and propellant mass loss of the thruster, yielding a per shot specific impulse. Competing design considerations affecting the performance of the thrust stand has lead to an optimized diagnostic tool capable of measuring total impulses up to 150 mN s with a resolution of 0.4 mN s and mass losses up to 18g with a resolution of 1 mg.

15. SUBJECT TERMS

16. SECURITY CLASSIFICATION OF:			17. LIMITATION OF ABSTRACT	18. NUMBER OF PAGES	19a. NAME OF RESPONSIBLE PERSON
					Dr. Andrew Ketsdever
a. REPORT	b. ABSTRACT	c. THIS PAGE	SAR	8	19b. TELEPHONE NUMBER *(include area code)*
Unclassified	**Unclassified**	**Unclassified**			N/A

Development of a Specific Impulse Balance for a Pulsed Capillary Discharge

T. C. Lilly*, A. P. Pancotti†
ERC Inc., 10. E. Saturn Blvd. Edwards AFB, CA 93524

A. D. Ketsdever‡, M. Young§, and J. A. Duncan**
Air Force Research Lab, 10. E. Saturn Blvd. Edwards AFB, CA 93524

A capillary discharge based pulsed plasma thruster is currently under development at the Air Force Research Laboratory. A torsion thrust stand has been developed to simultaneously measure the shot by shot total impulse and propellant mass loss of the thruster, yielding a per shot specific impulse. Competing design considerations affecting the performance of the thrust stand has lead to an optimized diagnostic tool capable of measuring total impulses up to 150 mN s with a resolution of 0.4 mN s and mass losses up to 18g with a resolution of 1 mg.

Nomenclature

α	=	$-C/2I$
β	=	$\sqrt{K/I-\alpha^2}$
C	=	torsion damping coefficient [N m s/rad]
δ_n	=	logarithmic decrement [n.d.]
ζ	=	damping ratio [n.d.]
F_c	=	steady state calibration force [N]
g_0	=	gravitational constant [m/s^2]
I	=	mass moment of inertia [N m s2/rad][kg m2/rad]
$\Im$	=	total impulse [N s]
I_{sp}	=	specific impulse [s]
K	=	torsion spring constant [N m/rad]
m_{prop}	=	mass of propellant [kg]
R_c	=	radial distance from pivot to calibration force [m]
R_s	=	radial distance from pivot to translation sensor [m]
R_t	=	radial distance from pivot to CD [m]
θ	=	rotational deflection of the thrust stand [rad]
X	=	linear displacement of the thrust stand, at the displacement sensor [m]
ω_0	=	natural frequency of the thrust stand [rad/s]
ω_d	=	damped frequency of the thrust stand [rad/s]

I. Introduction

A capillary discharge based coaxial, electrothermal pulsed plasma thruster (PPT) is currently under development at the Air Force Research Laboratory (AFRL) as a high efficiency alternative to more traditional ablative PPTs. The major drawback of the traditional ablative PPT is the propulsive efficiency. Even though specific impulses (I_{sp}) on the order of 1000 seconds have been achieved with ablative PPTs utilizing electromagnetic acceleration, the

---

* Coop Researcher, AIAA Student Member
† Research Engineer, AIAA Student Member
‡ Group Leader – Advanced Concepts, Propulsion Directorate, AIAA Senior Member
§ Senior Research Engineer – Advanced Concepts, Propulsion Directorate, AIAA Member
** Coop Researcher, Propulsion Directorate, AIAA Student Member

propulsive efficiencies of flight qualified thrusters typically remains below 10%.[1] Capillary discharges (CD) are relatively efficient sources of high density, high temperature plasmas which are being developed for a number of applications.[2,3,4] The capillary discharge being developed at AFRL consists of a high-density polyethylene (HDPE) capillary tube, a tungsten anode at the closed end of the tube, and a stainless-steel cathode at the open end. The anode is multi-segmented with differentially applied potentials to provide ignition. Capillary discharges maintain a resistive arc (generated at the anode) through the insulating capillary by the continual ablation of the HDPE wall material. Previous performance calculations have suggested that a capillary discharge based electrothermal PPT can achieve propulsive efficiencies of 30-40% even without nozzle expansion.[5] Additional studies indicate that nozzle expansion of the high pressure, high temperature plasma generated by the capillary discharge will increase the efficiency above 50%.[6] With the potential for vast improvement in efficiency, the capillary discharge, electrothermal PPT may be a strong candidate for satellite orbital insertion, attitude control, or station-keeping maneuvers.

In the present study, a diagnostic tool has been developed to investigate the applicability of a capillary discharge as an electrothermal PPT. A torsion thrust stand similar to that described by Ketsdever, et al.[7] has been designed to simultaneously measure the impulse and mass loss of the capillary discharge. The simultaneous nature of the developed technique will allow a per-pulse measurement of the discharge's specific impulse through the relation

$$I_{sp} = \frac{\Im}{m_{prop} g_0} \tag{1}$$

The technique is especially useful for propulsion systems that utilize solid propellant where a direct measurement of the propellant mass flow is extremely difficult. The thruster will be configured on the thrust stand such that the impulse generated by the discharge and the steady-state force generated by the propellant mass loss act in the same direction. The combined signal from these effects can then be decoupled to assess the ratio of the impulse to the weight of propellant expended yielding the specific impulse. The optimization for the thrust stand will be discussed in following sections.

A second thrust balance will then be configured in a manner similar to that described by D'Souza and Ketsdever[8] such that the stand will measure the time accurate shape and magnitude of the impulse delivered by the capillary discharge. Previous experimental measurements have shown that the typical capillary discharge pulse lasts several hundred micro-seconds.[5] By investigating the time accurate pulse by pulse impulse delivered by the capillary discharge, discharge efficiency may be dramatically improved. The time resolved impulse measurement (TRIM) technique involves investigating the equations of motion for the torsion thrust stand and recreating the forcing function from the measured time resolved displacement of the stand as described herein.

II. Thrust Stand Model and Analysis

The thrust stand was designed as a damped torsion force balance. The motion of the thrust stand can be modelled as an under-damped second order system described by

$$I\ddot{\theta}(t) + C\dot{\theta}(t) + K\theta(t) = M(t) \tag{2}$$

where $M(t)$ is the forcing moment. In order to model the expected motion of a potential design, eqn. (2) can be solved for θ such that[9]

$$\theta(t) = \frac{M_0}{K} + e^{\alpha t}\left[\left(\theta_0 - \frac{M_0}{K}\right)\cos(\beta t) + \left(\frac{\dot{\theta}_0 K - \alpha K\theta_0 + \alpha M_0}{K\beta}\right)\sin(\beta t)\right] \tag{3}$$

$$\dot{\theta}(t) = e^{\alpha t}\left[\dot{\theta}_0\cos(\beta t) + \left(\frac{I\alpha\dot{\theta}_0 - K\theta_0 + M_0}{I\beta}\right)\sin(\beta t)\right] \tag{4}$$

$$\ddot{\theta}(t) = e^{\alpha t}\left[\left(\frac{M_0 - C\dot{\theta}_0 - K\theta_0}{I}\right)\cos(\beta t) + \left(\frac{\alpha\left(M_0 - C\dot{\theta}_0 - K\theta_0\right) - K\dot{\theta}_0}{I\beta}\right)\sin(\beta t)\right] \tag{5}$$

where M_0 is a steady state forcing moment. For time dependant forcing moments, these equations can be discretized in time and solved over individual time steps forced by a constant forcing moment, $M_0 = \overline{M(t)}, t = t_0 \to t_0 + \Delta t$. Using the small angle approximation, $\sin\theta \approx \theta$ and the geometric relations $\theta = S/R$, where S is the arc swept by a point on the thrust stand, and $\sin\theta = X/R$, where X is the linear displacement of a point on the thrust stand, the rotational equations can be linearized at a radial distance, R. This yields a relation from eqn. (2) in terms of the signal from a displacement detector and the forcing function of

$$I\frac{\ddot{X}(t)}{R_s}+C\frac{\dot{X}(t)}{R_s}+K\frac{X(t)}{R_s}=F(t)R_t \tag{6}$$

As shown in Ref. 7, the simultaneous measurement of impulse and mass loss, where the ratio yields I_{sp}, is conducted by analyzing two aspects of the thrust stand's overall motion. The maximum deflection range of the thrust stand during a test is linear with the magnitude of the impulse. The change in the thrust stand position before and after the impulse applied is linear with the propellant mass loss. An example of these two measurements can be seen in Figure 1. The assumptions necessary for the linear relations to hold are that the pulse duration be much less than the stand's period and the mass loss has a known distribution as a function of radial distance from the pivot. If these conditions are satisfied, two sets of calibration runs, known impulse versus deflection range and known steady state force versus change in zero, are required to extract the absolute impulse magnitude and total mass loss from a single thrust stand trace.

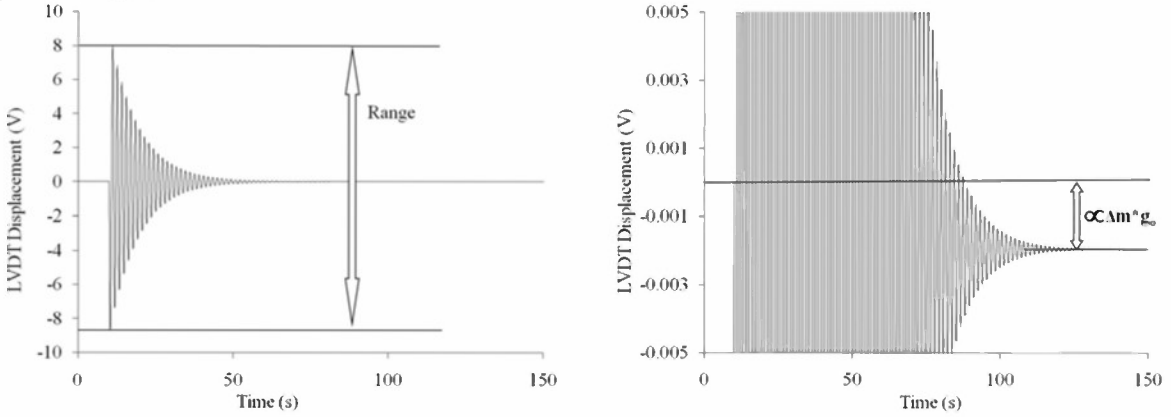

A **B**

Figure 1 Simulated trace of expected impulse and mass loss for the operational thruster.

For the measurement of the time dependant impulse shape (profile) using the TRIM method, Ref. 8 shows the validity of measuring the left hand side of eqn. (6) to reproduce the right hand side. In order to accomplish this, the constants, *K*, *C*, and *I*, must first be determined for the thrust stand. To find *K*, a steady state force is applied to the thrust stand. Given sufficient time to allow for the damping of oscillations, the limit of eqn. (6) as $t\rightarrow\infty$ becomes

$$K\frac{X}{R_s}=F_cR_c \tag{7}$$

The remaining two coefficients can be found by analyzing the measured period and the decay of the deflection amplitude as a function of time. First, a logarithmic decrement is defined as

$$\delta_n=\ln(X_i/X_{i+n}) \tag{8}$$

where *i* is a positive integer, and X_i and X_{i+n} are peak amplitudes, separated by *n* periods. The damping ratio is then given by

$$\zeta=\delta_n\Big/\sqrt{(n\cdot 2\pi)^2+\delta_n^{\,2}} \tag{9}$$

The measured frequency of the stand can be found from the measured period and related to the natural frequency by

$$\frac{2\pi}{T}=\omega_d=\omega_0\sqrt{1-\zeta^2} \tag{10}$$

where *T* is the measured period of the stand, and the mass moment of inertia and damping coefficients can be calculated as

$$I=\frac{K}{\omega_0^2} \tag{11}$$

$$C=2\zeta\sqrt{KI} \tag{12}$$

Therefore, the coefficients *I, C,* and *K* may be determined from any single test trace, or averaged over many test traces, resulting from a known, static, steady-state, calibration force. It follows that if the deflection, *X(t)*, resulting from a dynamic force, is measured on a stand with no significant change in *I, C,* or *K* during that time, then the time dependent function *F(t)*can be determined through equation (6).

III. Thrust Stand Design

The major components of the thrust stand are the rotational arm, damping magnets, flexure pivots (torsion springs), displacement sensor, and calibration system. The rotational arm contributes to the moment of inertia for the stand and provides a structure to attach thruster other components. The damping magnets are used as eddy current generators to damp the stand's motion and define the damping coefficient for the stand. The torsion springs contribute to the spring constant by providing the restoring force. The displacement sensor measures the linear motion of the stand and defines the limits of the stand's motion as well as the precision of the measurements. The calibration system provides a known steady state force and transient impulse to the stand and defines the useful range of the stand's accuracy. The major components of the stand can be seen in Figure 2.

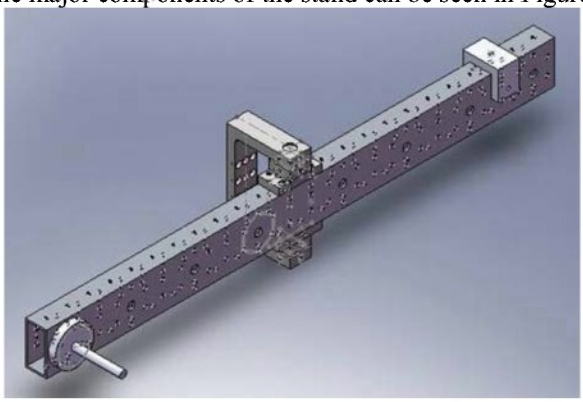

Figure 2 CAD drawing of first iteration thrust stand in the impulse profile measurement configuration.

Special consideration must be given to a choice in displacement sensors since the CD involves strong electromagnetic fields during the discharge. Such fields will interfere with any locally mounted electronic force sensors, such as piezo based load cells. This requires that a non-electronic or remote sensing sensor be used. This interference is only a factor during the thruster firing. Thus, for sensors that recover from such interference quickly the effect is negligible for I_{sp} measurements. Linear voltage differential transformers (LVDTs) have been successfully implemented for previous iterations of similar thrust stands.[7,8] These sensors have an advertised linearity of $\leq 0.25\%$. For a 2.5 mm full range device, this translates to a linear accuracy of better than 6.25 μm. The linear range and accuracy of the detector, for a given thrust stand configuration, directly set the maximum impulse and minimum mass loss able to be resolved by the thrust stand. Unfortunately, LVDTs have an inherent excitation frequency on the order of 10^3 Hz, which limits the response time and makes it unfeasible for time accurate profile measurements of the CD, which has a pulse width on the order of 300 μs.[5] For the time accurate profile measurements, one alternative to the LVDT is an interferometric system. One particular laserinterferometric vibrometer has an advertised displacement range of ±20 mm, a resolution on the order of 0.3 nm and a sampling rate of up to 10^6 Hz.[††] In addition, an interferometric system is not influenced by the EMI given that the working distance of the interferometer allows the electronics to be mounted outside the test cell.

In order to correlate position measurements with known forces and impulses, the stand must be calibrated in the same configuration that the thruster testing is conducted. The most straightforward system is to place calibrated weights on the stand to create a known force. Unfortunately, this method is not easily replicated for in-situ vacuum calibration. Previous iterations of thrust stands have used electrostatic combs to generate repeatable and known attractive forces.[10] Unfortunately, the maximum steady state force generated by such a system has only been demonstrated on the order of 10^{-6}-10^{-3} N. With a thrust stand period on the order of 1 second, impulses on the order of 10^{-7}-10^{-4} N s are all that a comparably sized system could impart and still adhere to a pulse width much less than the stand period. This is too small for an expected CD impulse magnitude of 10^{-1} N s^5. To cover the lower region of impulse calibration and allow for steady state force calibration, a larger scaled electrostatic comb system has been designed and built to impart up to $5x10^{-2}$ N of force to the thrust stand. To cover the higher region of impulse calibration, a piezoelectric impact hammer will be implemented to calibrate in the 10^{-4}-10^{1} N s range. Such a system offers a much higher range of calibration values, but may not be easy to implement in a vacuum environment.

[††] SIOS, SP-Series plane-mirror miniature interferometer, http://sios.de/ENGLISCH/PRODUKTE/SP_E_FOT.PDF

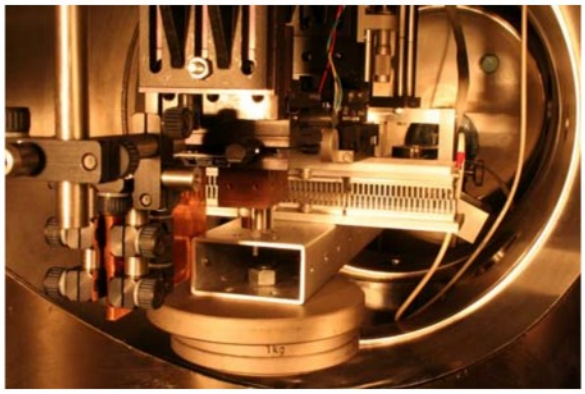

Figure 3 Experimental thrust stand, calibration system, LVDT, and magnetic damping.

When choosing a set of flexure pivots for the stand, the primary concern for the specific impulse measurement is that the change in beginning and ending positions due to CD mass loss is large enough to be resolved by the displacement sensor and ancillary acquisition hardware. For the steady state condition before and after the CD discharge, the displacement of the thrust stand is only dependant on the magnitude and position of the mass loss and the K value of the stand. Figure 4(A) shows the expected LVDT reading on the designed thrust stand shown in Figure 3 for a 12 mg mass loss, the amount predicted by the CD model in Ref. 6. Given a data acquisition hardware resolution of better than 1 mV, any of the spring constants in the plotted range would be able to resolve a single shot mass loss measurement, with a preference for larger displacements going to smaller spring constants. In addition to the displacement due to mass loss, the spring constant, as well as the moment of inertia, affects the maximum displacement range of the thrust stand for a given impulse. The displacement range decreases with increasing spring constant and moment of inertia. Since there is a diminishing return for adding mass to the thrust stand, a preference for smaller displacement ranges within the range of the displacement sensor gives preference to higher spring constants. This leads to a trade that yields an optimum value for the spring constant when balancing between the sensitivity needed for the mass loss measurements and the restoring force needed for the total impulse measurements. Figure 4(B) shows the effect of the moment of inertia on the maximum displacement range of the thrust stand for several values of the spring constant.

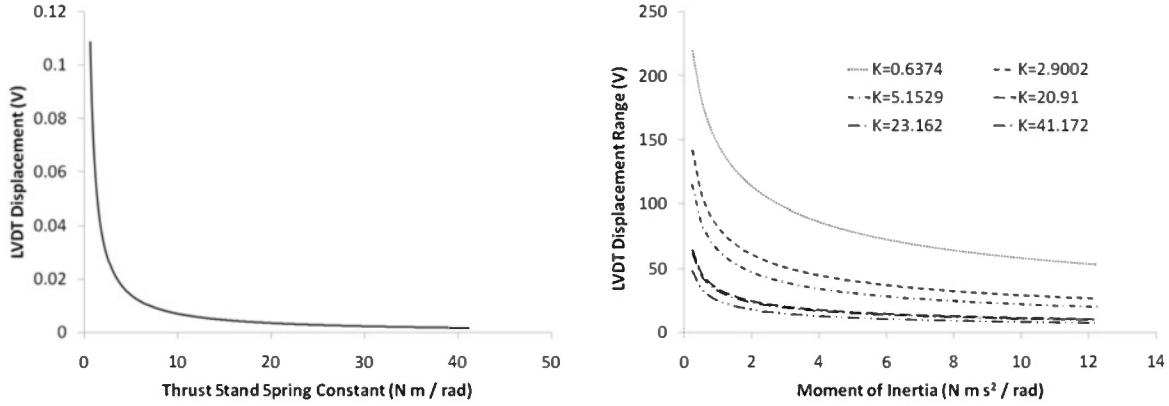

(A) **(B)**

Figure 4 (A) Thrust stand deflection vs. K and (B) thrust stand deflection range vs. I for multiple K.

IV. Results and Discussion

As a iterative first step to I_{sp} measurements, a 91.44 cm thrust stand, calibrated by electrostatic combs and sensed by a 2.5 mm full range LVDT, was built. This iteration represented only the elements required for a working thrust stand. The model coefficients for the thrust stand can be seen in Table 1. The measured K value matches the advertised unloaded spring constant from the manufacturer (published as ±10%) within 1.5%. Given these values and the expected CD impulse, this iteration had a moment of inertia which would yield an LVDT deflection range, from Figure 4, much larger than the useful range of the sensor. Changing the magnets or torsion springs (thus C or K) yields a discrete set of combinations. However, altering the moment of inertia offers near continuous possibility by simply adding mass to the rotational arm. Thus the simplest way of reducing the deflection range for a given

impulse is to increase the mass moment of inertia. The resultant characteristics for the optimized stand are also given in Table 1.

Thrust Stand	1st Iteration	Operational
K	41.75	36.22
C	0.191	0.428
I	0.245	1.988

Table 1 Thrust stand characteristics

As verification for the thrust stand model discussed in the previous section, equations (3) and (4) were solved for an experimentally tested 7.25×10^{-4} N s calibration impulse. The comparison between the experimental first iteration and operational thrust stands and the model can be seen in Figure 5, with the model shifted to account for an arbitrary DC offset in the experiment. Note that the experimental and the model line data almost completely coincide. The change in I and observed change in K are properly reflected in a change in measured period and maximum deflection range between the two iterations.

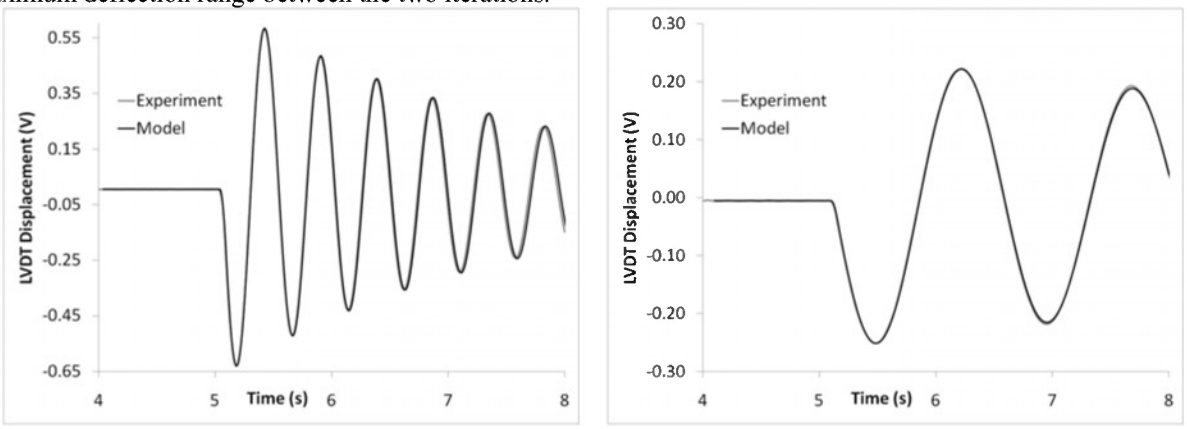

(A) **(B)**

Figure 5 Model comparison between (A) first iteration and (B) operational thrust stands for a 3.63 mNs impulse.

In order to test the CD attachment, data acquisition and control, and the power transfer connections, the CD was attached to the first iteration thrust stand. Because the CD at operational power levels would result in an impulse larger than the first iteration thrust stand would be able to measure, the CD was operated at very low power levels. The displacement range measured by the LVDT on this stand versus the voltage potential on the discharge capacitor bank can be seen in Figure 6. From Ref. 6, the total impulse should increase with an increase in capacitor potential, a trend that is reflected by the increase in measured deflection range.

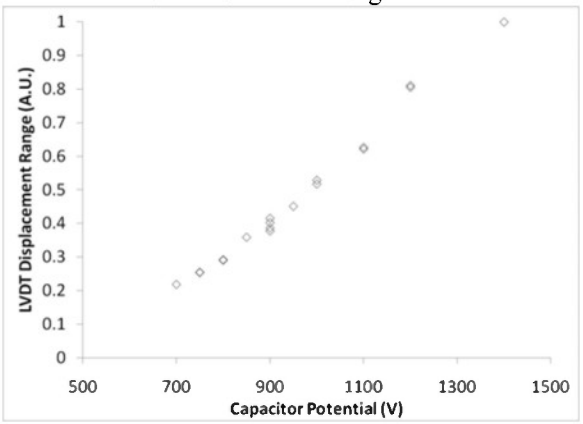

Figure 6 Thrust stand displacement range vs. CD capacitor potential.

While operating at its full discharge potential, the CD is expected to produce $\approx 10^{-1}$ N s of impulse with a propellant mass of 12 mg[6]. The expected output of the LVDT for such a firing on the operational thrust stand can be seen in Figure 1. This represents the operational levels for which the thrust stand was designed and optimized. If experimental values are found to be significantly different than those predicted by the CD model, the thrust stand

maintains the flexibility to be easily optimized for a large range of total impulse values by variations in the mass moment of inertia, spring constant or damping coefficient.

Acknowledgments

This work was supported by the Advanced Concepts Group at the Propulsion Directorate of the Air Force Research Laboratory at Edwards AFB, CA.

References

[1] Kamhawi, H., Arrington, L., Pencil, E., and Haag, T., "Performance Evaluation of a High Energy Density Pulsed Plasma Thruster," AIAA paper 2005-3695, 2005.

[2] Zigler, A., Ehrlich, Y., Cohen, C., Krall, J., and Sprangle, P., "Optical Guiding of High-Intensity Laser Pulsed in a Long Plasma Channel Formed by a Slow Capillary Discharge," *J. Opt. Soc. Am. B*, 13, 1996, pp. 68-71.

[3] Lee, R. and Zigler, A., "Multiple Pulse Laser Excitation of a Capillary Discharge," Appl. *Phys. Lett.*, Vol. 53, No. 21, 1998, pp. 2028-2029.

[4] Powell, J. and Zielinski, A., "Theory and Experiment for an Ablating Capillary Discharge and Application to Electrothermal-Chemical Guns," Army Ballistic Research Laboratory, Report BRL-TR-3355, June 1992.

[5] Cambier, J., Young, M., Pekker, L., and Pancotti, A., "Capillary Discharge Based Pulsed Plasma Thrusters," *International Electric Propulsion Conference*, IEPC-2007-238, 2007.

[6] Pekker, L. and Cambier, J., "A Model of Ablative Capillary Discharge," IHTC-13, Sydney, Australia, Aug. 13-18, 2006.

[7] Ketsdever, A., Lee, R., and D'Souza, B., "Thrust Stand Micro-Mass Balance for the Direct Measurement of Specific Impulse," *J. Prop. and Power*, accepted for publication. See also, AIAA paper 2007-5300, 2007.

[8] D'Souza, B. and Ketsdever, A., "Investigation of Time-Dependent Forces on a Nano-Newton-Second Impulse Balance," *Rev. Sci. Instrum.*, Vol. 76, No. 1, 2005, pp. 015105 1-10.

[9] Vierck, R. K., *Vibration Analysis* (Thomas Y. Crowell, New York, 1979).

[10] Selden N. P. and Ketsdever A. D., Comparison of force balance calibration techniques for the nano-Newton range, *Rev. Sci. Instrum.* **74** 5249–54, 2003